Emergence of collective self-oscillations in minimal lattice models with feedback

Dmitry Sinelshchikov [1,2,7] Anna Poggialini [3,4] Maria Francesca Abbate,[5,6] and Daniele De Martino [1,7]

[1]*Biofisika Institutua (UPV/EHU, CSIC) and Fundación Biofísica Bizkaia, Leioa E-48940, Spain*
[2]*HSE University, 34 Tallinskaya Street, 123458 Moscow, Russian Federation*
[3]*Dipartimento di Fisica, Sapienza Università di Roma, P.le A. Moro, 2, I-00185 Rome, Italy*
[4]*'Enrico Fermi' Research Center (CREF), Via Panisperna 89A, 00184 Rome, Italy*
[5]*Digital Biologics Platform (DBxP) Site Lead France, Large Mol. Res. Platform at Sanofi*
[6]*Laboratoire de physique de l'École normale supérieure, CNRS, PSL University, Sorbonne Université, and Université de Paris, 24 rue Lhomond, 75005 Paris, France*
[7]*Ikerbasque Foundation, Bilbao 48013, Spain*

(Received 2 June 2023; accepted 11 September 2023; published 6 October 2023)

The emergence of collective oscillations and synchronization is a widespread phenomenon in complex systems. While widely studied in the setting of dynamical systems, this phenomenon is not well understood in the context of out-of-equilibrium phase transitions in many-body systems. Here we consider three classical lattice models, namely the Ising, the Blume-Capel, and the Potts models, provided with a feedback among the order and control parameters. With the help of the linear response theory we derive low-dimensional nonlinear dynamical systems for mean-field cases. These dynamical systems quantitatively reproduce many-body stochastic simulations. In general, we find that the usual equilibrium phase transitions are taken over by more complex bifurcations where nonlinear collective self-oscillations emerge, a behavior that we illustrate by the feedback Landau theory. For the case of the Ising model, we obtain that the bifurcation that takes over the critical point is nontrivial in finite dimensions. Namely, we provide numerical evidence that in two dimensions the most probable value of a cycle's amplitude follows the Onsager law for slow feedback. We illustrate multistability for the case of discontinuously emerging oscillations in the Blume-Capel model, whose tricritical point is substituted by the Bautin bifurcation. For the Potts model with $q = 3$ colors we highlight the appearance of two mirror stable limit cycles at a bifurcation line and characterize the onset of chaotic oscillations that emerge at low temperature through either the Feigenbaum cascade of period doubling or the Afraimovich-Shilnikov scenario of a torus destruction. We also demonstrate that entropy production singularities as a function of the temperature correspond to qualitative change in the spectrum of Lyapunov exponents. Our results show that mean-field collective behavior can be described by the bifurcation theory of low-dimensional dynamical systems, which paves the way for the definition of universality classes of collective oscillations.

DOI: 10.1103/PhysRevE.108.044204

I. INTRODUCTION

The emergence of oscillations in complex systems is a widespread phenomenon that appears across various fields of science. For example, oscillatory behavior can arise in biological systems, chemical reactions, and mechanical systems (see, e.g., Refs. [1–3]). These oscillations often manifest themselves as collective behavior, where individual components interact and synchronize their activities over time, and studying underlying mechanisms is an important problem for understanding of complex systems.

One theoretical framework that could potentially shed light on the emergence of oscillations is the one of nonequilibrium phase transitions in statistical physics. While a deep and powerful physical theory underlies the classification of equilibrium critical points, this same task has not been yet achieved for out-of-equilibrium phase transitions, in particular for the emergence of collective oscillations and synchronization phenomena. After the work of Landau and coworkers [4] it was realized that the plethora of experimental data on continuous phase transitions could be unified on the basis of the symmetries of the underlying interacting degrees of freedom. One of the paradigmatic examples is the equivalence of critical exponents for liquid-gas and paramagnetic-ferromagnetic phase transitions [4]. This led to the concept of universality classes [5], that is connected to field theories and the renormalization group [6].

Recent works try to establish general and universal concepts in out-of-equilibrium phenomena: example range from the proposal of the directed percolation universality class, including reaction-diffusion and epidemic spreading [7] to the modeling of nonreciprocal phase transitions [8]. Moreover, studies of synchronization phenomena in many-body systems stands out as a very active area of research taking into account its importance for modeling complex systems [9–11]. One of the difficulties related to out-of-equilibrium systems is a lack of general variational principles and reference free energy landscapes. Consequently, a great majority of the studied models are variations of the Kuramoto model [12–16], where the interacting units are postulated as oscillators at the outset and their phase coherence is analyzed. Dynamical phase transitions in classical lattice models has been studied as well, by postulating oscillating control parameters

(external fields) and considering the synchronization properties of the associated order parameters, including the Ising [17,18], the Blume-Capel [19], and the Potts models [20], and the Ginzburg-Landau theory [21].

Alternatively, in the very seminal works on this topic the emergent character of oscillations (thus, called self-oscillations) without the need to postulate them was remarked [1,2,22]. This area has been considerably developed during recent years and appearance and synchronization of periodic, quasiperiodic, chaotic, and even hyperchaotic self-sustained oscillations in mechanical, physical, and biological models, described by dynamical systems, has been demonstrated and studied [2,23–26]. Moreover, the importance of bifurcations or their sequences leading to the onset of regular or chaotic self-oscillations has been shown in numerous works (see, e.g., Refs. [2,27–31]). Therefore, following this route, in this work we study scenarios of the emergence of collective oscillations in minimal spin lattice models [32] in presence of a feedback between the control and the order parameter trying to enforce homeostasis in the symmetric phase. We show that the feedback can generically put these systems out-of-equilibrium, in particular triggering coherent collective oscillations. The static counterparts of these system have a well defined free energy landscape and an important question is to what extent the latter can provide insights into the actual dynamics. We will illustrate this mechanism in the Landau theory with feedback that gets mapped into nonlinear Van der Pol-type oscillators. Then we will explore it concretely in the Ising, Blume-Capel, and Potts models.

We demonstrate the onset of collective periodic oscillations in the Ising model with feedback after the corresponding mean-field dynamical system undergoes the Andronov-Hopf bifurcation. We also obtain that for slow feedback the most probable value of a cycle's amplitude follows the Onsager law. For the Blume-Capel model we show that there is the Bautin bifurcation in the mean-field dynamical system that corresponds to the tricritical point in its collective counterpart. The existence of such bifurcation naturally leads to the presence of multistability in both mean-field and full microscopic models, which is numerically illustrated. As far as the Potts model with three colors in concerned, we observe even more complex behavior. For the regions with low feedback and high temperature we obtain that there is the onset of self-oscillations in the way similar to the Blume-Capel model and again with a region of multistability in the parameters' space. However, for bigger feedback we demonstrate that the behavior is much more complex and quasiperiodic, and chaotic oscillations emerge in both mean-field and microscopic models. Two bifurcation scenarios for the onset of chaotic oscillations are observed: the Feigenbaum cascade of period doubling and the Afraimovich-Shilnikov scenario of torus destruction. These results manifest that limit cycles bifurcations, complex bifurcation scenarios, and collective quasiperiodic and chaotic oscillations can be observed in full microscopic models. Furthermore, we demonstrate that the low-dimensional dynamical systems obtained via linear response provide for an effective mean-field description of the complex behavior of the full system. On the whole, we believe that this work provides a way of understanding of the onset of the complex collective behavior in out-of-equilibrium systems.

The rest of the paper is organized as follows. In the next section we present our main results on collective oscillations in feedback lattice models. In Sec. II A we briefly discuss the feedback Landau theory. Section II B is devoted to Ising model where we deal with the dynamics of the system in a fully connected geometry with a general linear feedback and in a two-dimensional (2D) square lattice. The subsequent Sec. II C presents our results for the Blume-Capel model, which is an extension of the Ising model in presence of vacancies. Section II D is focused on the Potts model with $q = 3$ colors with feedback and we summarize and discuss our findings in Sec. III.

II. RESULTS

A. Feedback Landau theory

Here we generalize the results presented in Ref. [33] on the effect of the presence of feedback in the Landau theory with higher-order relevant terms. Let us consider the expansion of the free energy density up to the sixth power of a scalar order parameter ϕ

$$\mathcal{L}(\phi) = -h\phi - \frac{\beta - 1}{2}\phi^2 + \frac{a}{4}\phi^4 + \frac{b}{6}\phi^6, \tag{1}$$

where h is the external field, β is the inverse temperature and a, b are arbitrary real parameters.

Upon considering a negative feedback between h and ϕ aiming at controlling the system into the symmetric phase, by linear response we have, upon neglecting noise in the thermodynamic limit, the dynamical system

$$\begin{aligned} \dot{\phi} &= -\frac{\partial \mathcal{L}}{\partial \phi} = h + (\beta - 1)\phi - a\phi^3 - b\phi^5, \\ \dot{h} &= -c\phi. \end{aligned} \tag{2}$$

The system has an equilibrium state at $(\phi = 0, h = 0)$ whose stability is associated to the eigenvalues of the Jacobian of the linearized system

$$\lambda_{\pm} = \frac{\beta - 1 \pm \sqrt{(\beta - 1)^2 - 4c}}{2}. \tag{3}$$

Thus, it is stable iff $\beta < 1$, being a stable focus if $4c > (\beta - 1)^2$ and a stable node otherwise. Since the system is confined (as it can be seen by looking to the gradient at the boundary of the square with vertex), at $\beta_c = 1$ the eigenvalues are purely imaginary and the real part changes sign and the system is undergoing the Andronov-Hopf bifurcation with emergent nonlinear oscillations.

The character of the bifurcation can be assessed by calculating the first Lyapunov coefficient (see, e.g., Refs. [23,27]), which in this case is $l_1 = -\frac{3}{8}a$. Thus, we have that at $a = 0$ the bifurcation of the system changes from supercritical to subcritical behavior with a discontinuous onset of oscillations. This analysis seems to support an equivalence between the character of the Andronov-Hopf bifurcation and the one of the underlying equilibrium static transition. If that would be the case the supercritical emergence corresponds to a second-order phase transition and subcritical emergence corresponds to a first-order phase transition, where by the nth order we mean the order of singularity of the free energy function, in

particular, independently of the feedback strength c. We will show that this Landau feedback theory captures the qualitative behavior of the Ising and Blume-Capel models while it fails to do so for the Potts model as soon as $q = 3$.

B. Feedback Ising model

We will extend in this section the results of Ref. [33] analytically in presence of a general linear control and numerically in finite dimension. We consider the Ising model, i.e., a model of Z_2 spins $s_i = \pm 1$ variables sitting on the nodes of a lattice graph whose Hamiltonian is

$$H = -J \sum_{\langle i,j \rangle} s_i s_j - h \sum_i s_i, \tag{4}$$

where the bracket in the first sum stands for the graph bonds and we indicate with J and h the interaction strength and the external magnetic field, respectively. Upon generalizing from [33] we apply a negative feedback between the instantaneous magnetization $m = \frac{1}{N}\sum_i s_i$ and the external magnetic field h, with the aim of setting the former to a prescribed value m_0, $|m_0| < 1$, which is a parameter of the system. The free energy is obtained from the partition function [32]

$$Z = \sum_{\{\vec{s}\}} e^{-\beta H} = \int dm e^{-N\beta f(m)}. \tag{5}$$

This calculation for general arbitrary graphs would require to solve difficult combinatorial problems: e.g., for the Ising model it would require an exhaustive enumeration of the loops in the graph, a task that was done by Onsager for the 2D square lattice and it is still an unsolved problem for the 3D case [32]. A simple mean-field method consists in substituting the sum over the bonds with a sum over all the possible pairs (that is equivalent to a fully connected graph), i.e.,

$$\sum_{\langle i,j \rangle} \to \frac{1}{N} \sum_{i,j}, \tag{6}$$

where the factor $1/N$ guarantees that the energy is extensive. In this approximation (Curie-Weiss), in the limit of large N the free energy of the system is

$$f = -\frac{J}{2} m^2 + \frac{1}{\beta} \log\{\cosh[\beta(Jm + h)]\}. \tag{7}$$

In regard to the dynamics we will assume linear response, i.e., that the time derivative of the magnetization is proportional to the gradient of the free energy function [36]. Upon considering the feedback the system is described by the equations

$$\dot{m} = -m + \tanh[\beta(Jm + h)], \quad \dot{h} = -c(m - m_0). \tag{8}$$

This system admits the only stationary point

$$m_s = m_0, \quad h_s = \operatorname{atanh}(m_0)/\beta - Jm_0, \tag{9}$$

whose linear stability can be assessed studying the eigenvalues of the Jacobian matrix ($\beta_2 = \beta J[1 - m_0^2]$)

$$\lambda_\pm = \frac{\beta_2 - 1 \pm \sqrt{(\beta_2 - 1)^2 - 4\beta_2 c}}{2}. \tag{10}$$

The equilibrium point is stable if and only if $\beta < \beta_c = \frac{1}{J(1-m_0^2)}$ and its character changes from a node to a focus (dynamical crossover), where eigenvalues develop an imaginary part, if $c > \frac{(\beta/\beta_c - 1)^2}{4\beta/\beta_c} J$. In the latter case the loss of stability at $\beta = \beta_c$ (phase transition) implies the Andronov-Hopf bifurcation triggering self-oscillations. The character of the bifurcation, supercritical (continuous) or subcritical (discontinuous) can be assessed from the sign of the first Lyapunov coefficient l_1. For (8) at $\beta = \beta_c$ it is

$$l_1 = -\frac{c + J}{(cJ)^{3/2}\left(1 - m_0^2\right)}. \tag{11}$$

Consequently, we see that the Andoronov-Hopf bifurcation is supercritical provided that $|m_0| < 1$.

Beyond the critical point, an approximate analytical solution can be worked out for $\beta >\sim \beta_c$ (harmonic oscillations) by a two-time expansion [2], if we call $\epsilon = \beta - \beta_c$ we have

$$m - m_0 \sim \sqrt{\epsilon} \cos\left(\left(1 + \tfrac{1}{2}\epsilon\right)\sqrt{c}t + \phi_0\right). \tag{12}$$

On the other hand, in the limit $\beta \to \infty$, where the system is performing relaxational oscillations, the equations are piecewise linear and the shape of the limit cycle can be found by matching the boundary conditions of solutions in half-spaces [1]. Notice that the two regimes differ qualitatively by the fact that the quasiharmonic oscillations are centered in m_0 and pass equal time up and down from this value, while in the relaxational regime they are centered in 0 and pass uneven times upon having positive and negative values such that their average will be in the end m_0. These results are in quantitative agreement with numerical simulations of the lattice system in a fully connected geometry as we show in Fig. 1 where we recapitulate the behavior in a phase diagram in the plane (m_0, β). The mean-field approximation of the static Ising model is known to capture qualitatively the behavior of the system in finite-dimensional geometry, but it fails quantitatively on the surroundings of the critical point. The study of the Ising model in finite dimension is arguably one of the most important areas in statistical physics, touching upon issues related to field theories and renormalization. One of the most important and earlier results, due to Onsager [37] and achieved by combinatorial counting, is an analytical solution for the system in a 2D square lattice where we have the formula for the spontaneous magnetization:

$$m = (1 - \sinh^{-4} 2\beta)^{1/8}, \tag{13}$$

valid for

$$\beta > \beta_c = \tfrac{1}{2}\log(1 + \sqrt{2}). \tag{14}$$

The analogy with the static counterpart would suggest that for the case with feedback in finite dimension we could have a limit cycle emerging with a nontrivial exponent and we explore this issue by numerically studying the Ising model with feedback in a 2D square lattice graph.

The corresponding results are shown in Fig. 2. Simulations have been performed for a system with $N = 10^4$ spins, for a neutral $m_0 = 0$ and slow $c = 10^{-4}$ feedback. First of all we provide evidence [see Figs. 2(a) and 2(b)] that for $\beta > \beta_c$ a limit cycle emerges whereas for $\beta < \beta_c$ the dynamics is

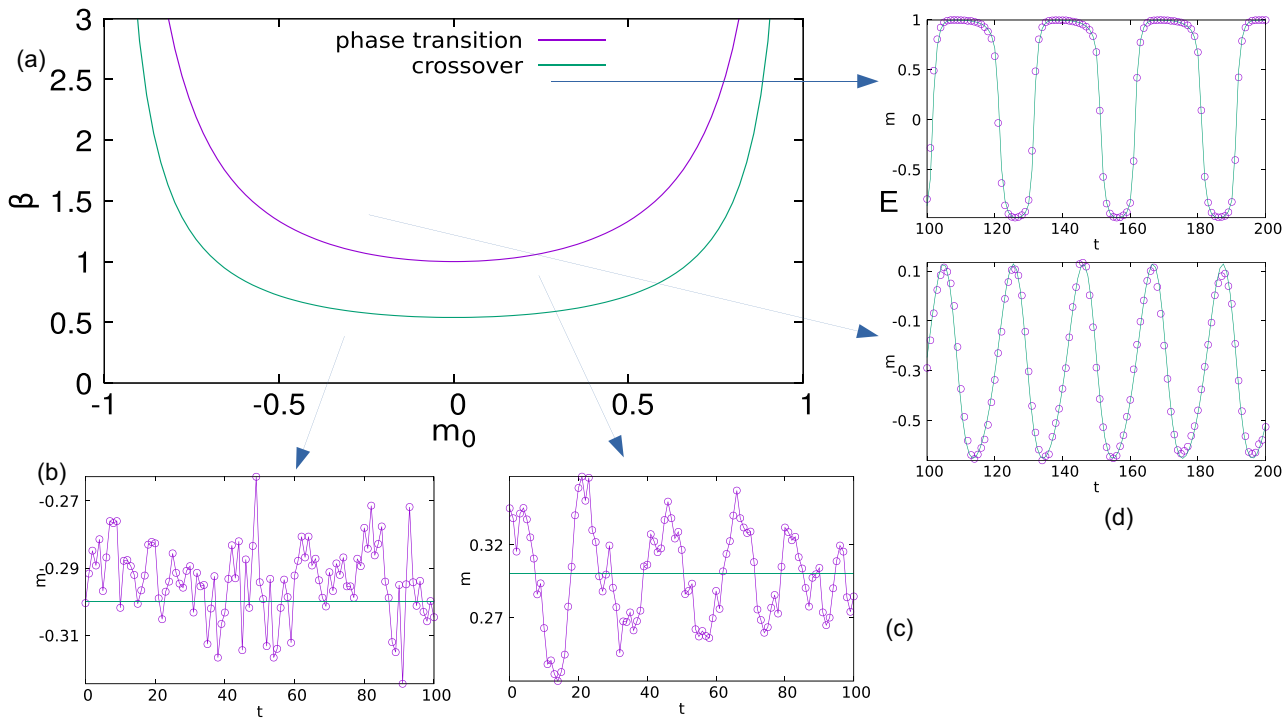

FIG. 1. (a) Mean-field phase diagram of the feedback Ising model in the plane (m_0, β) for $J = 1$, $c = 0.1$, both the critical line and the dynamical crossover line are highlighted. (b)–(e) magnetization time traces of the system simulated on a fully connected geometry in four different points corresponding to different dynamical behavior: full many-body stochastic simulations (violet dots, system size $N = 10^4$ spins) versus numerical solution of the low-dimensional ODEs (green line). (b) $m_0 = -0.3$, $\beta = 0.25$; (c) $m_0 = 0.3$, $\beta = 1$; (d) $m_0 = -0.3$, $\beta = 1.25$; (e) $m_0 = 0.3$, $\beta = 2.5$. Simulations are made via the Metropolis-Hastings method [34,35].

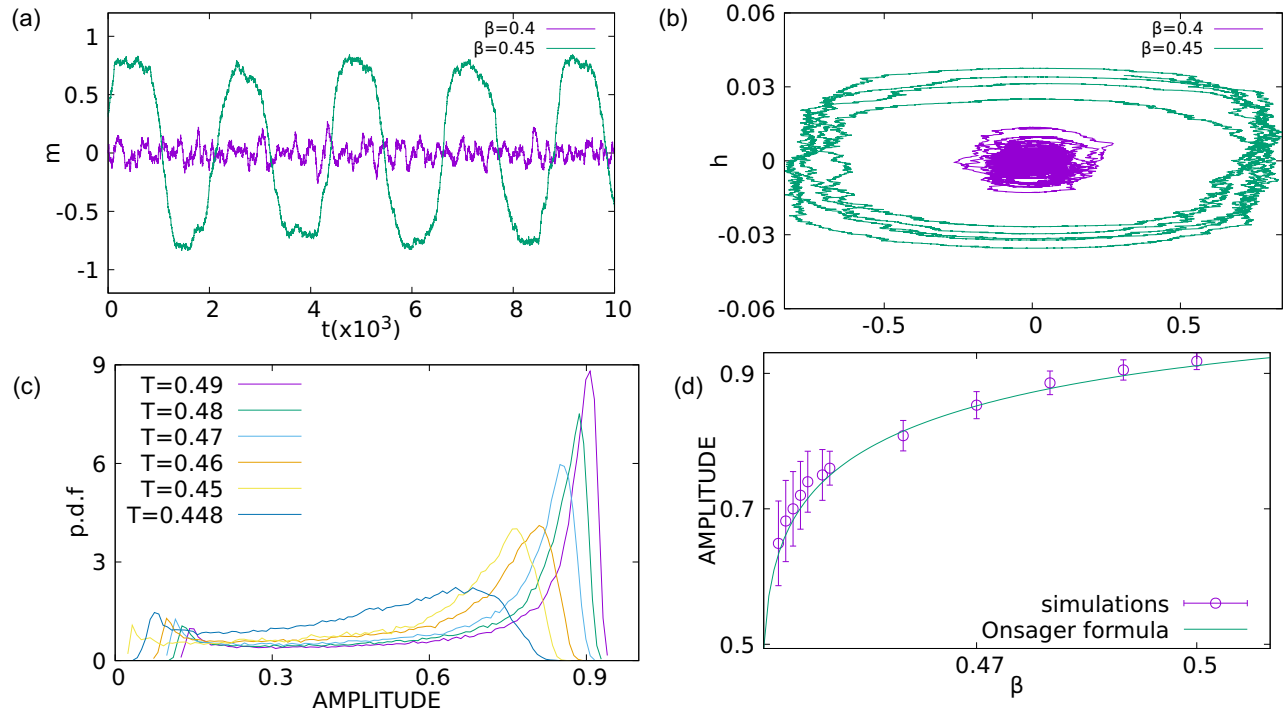

FIG. 2. Simulations of the feedback Ising model on a 2D square lattice; system size $N = 10^4$ spins, feedback strength $c = 10^{-4}$. (a) Magnetization as function of time $m(t)$ for $\beta = 0.47, 0.45$. (b) Trajectories in the phase plane (m, h) for $\beta = 0.47, 0.45$. (c) Histograms of the probability distribution of the limit cycle amplitude at several βs. (d) Most probable limit cycle amplitude as function of $\beta - \beta_c$ compared with Onsager formula and $\beta_c = \frac{\log(1+\sqrt{2})}{2}$. Simulations are made via the Metropolis-Hastings method [34,35].

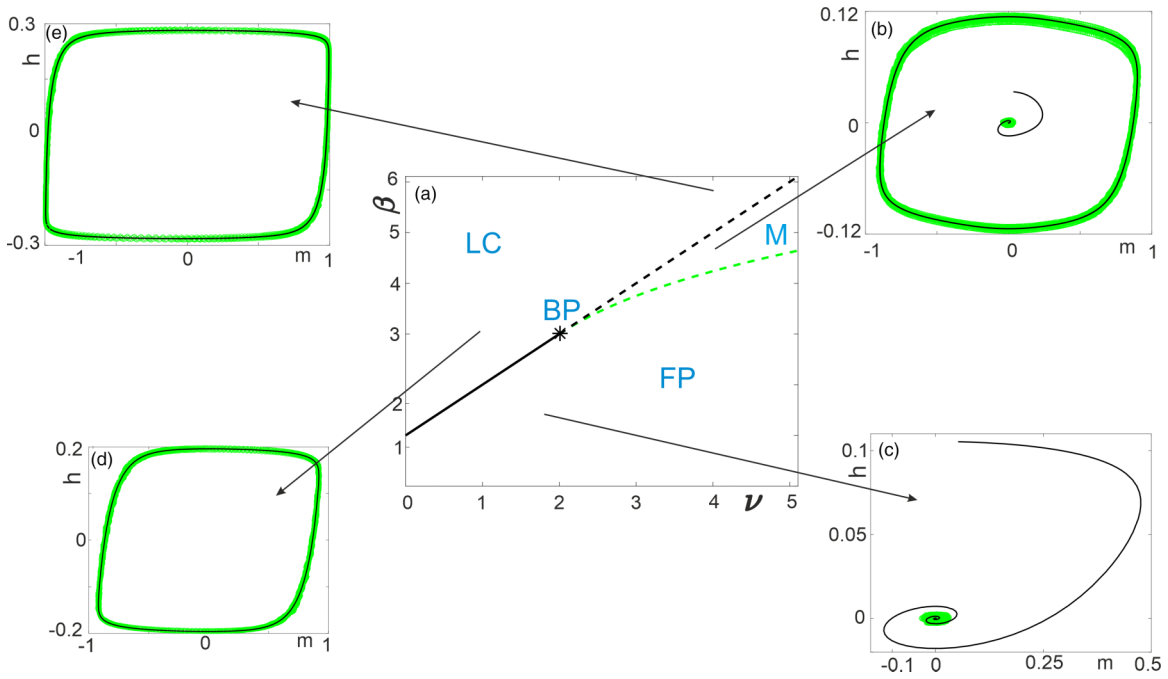

FIG. 3. Sketch of the behavior of system (18) nearby the Bautin bifurcation point. (a) Bifurcation diagram for (18), where black line is the line of the Andronov-Hopf bifurcation and the green one is the line of saddle-node bifurcation of limit cycles. Phase portraits of solutions of (18) nearby bifurcation point (black line) and the results full microscopic stochastic simulations in the fully connected model with $N = 10^4$ spins (green dots). (b) Confirmation of multistability. (c) Stable fixed point. (d), (e) Different limit cycles. Simulations are made via Metropolis-Hastings method [34,35].

relaxing into fixed point with $\beta_c \simeq 0.44$ consistent with the analytical value.

We investigate in further details this aspect by quantitatively comparing the limit cycle amplitude with the Onsager formula. This has been done by observing the trajectory of the system in the phase space (m, h) and extracting the radial coordinate. The distribution of the latter is shown in Fig. 2(c) and for $\beta > \beta_c$ it develops a second peak in correspondence with the formation of a limit cycle. The value at the peak has been evaluated against β in Fig. 2(d) and the trend is compared with the Onsager formula: we find a good agreement within errors, evaluated as the width at half-maximum.

C. Feedback Blume-Capel model

Here we consider a generalization of the Ising model in presence of vacancies, i.e., the spin variables admit the null value $s_i = 0, \pm 1$ and the Hamiltonian has an additional term counting the number of filled sites whose average is fixed by the chemical potential Δ:

$$H = -J \sum_{\langle i,j \rangle} s_i s_j - h \sum_i s_i + \Delta \sum_i s_i^2. \tag{15}$$

The static free energy of the system in a fully connected geometry can be calculated analytically [38]

$$f = -\frac{J}{2} m^2 + \frac{1}{\beta} \log(1 + 2\cosh(\beta(Jm + h)) e^{\beta\Delta}). \tag{16}$$

The system with feedback fulfills the approximate equations

$$\dot{m} = -m + \frac{\sinh(\beta(Jm + h))}{\frac{e^{\beta\Delta}}{2} + \cosh(\beta(Jm + h))},$$
$$\dot{h} = -cm. \tag{17}$$

In order to simplify analysis of (17) we introduce new variables $m' = \beta J m$ and $h' = \beta h$. We also redefine the parameters as follows: $c' = c/J > 0$, $\beta' = J\beta > 0$, $\Delta' = \Delta/J$ and $e^{\beta'\Delta'} = 2\nu > 0$. As a result, from (17) we obtain (the primes are omitted)

$$\dot{m} = -m + \frac{\beta \sinh(m + h)}{\nu + \cosh(m + h)}, \quad \dot{h} = -cm. \tag{18}$$

It is clear that the origin $O = (0, 0)$ is the fixed point of (18). We begin with the analysis of codimension one bifurcation in (18) and suppose that the β is the control parameter and c and ν have some fixed values. The Jacobi matrix for (18) at O is

$$\mathcal{J} = \begin{pmatrix} \frac{\beta - \nu - 1}{\nu + 1} & \frac{\beta}{\nu + 1} \\ -c & 0 \end{pmatrix}. \tag{19}$$

Consequently, the eigenvalues of (19) can be expressed via

$$\sigma = \mathrm{tr}(\mathcal{J}) = \frac{\beta - \nu - 1}{\nu + 1}, \quad \delta = \det \mathcal{J} = \frac{\beta c}{\nu + 1}, \tag{20}$$

as follows:

$$\lambda_{1,2} = \tfrac{1}{2}(\sigma \pm \sqrt{\sigma^2 - 4\delta}). \tag{21}$$

First, we are interested in the Andronov-Hopf bifurcation and, hence, we assume that $4\delta - \sigma^2 > 0$, so that we have

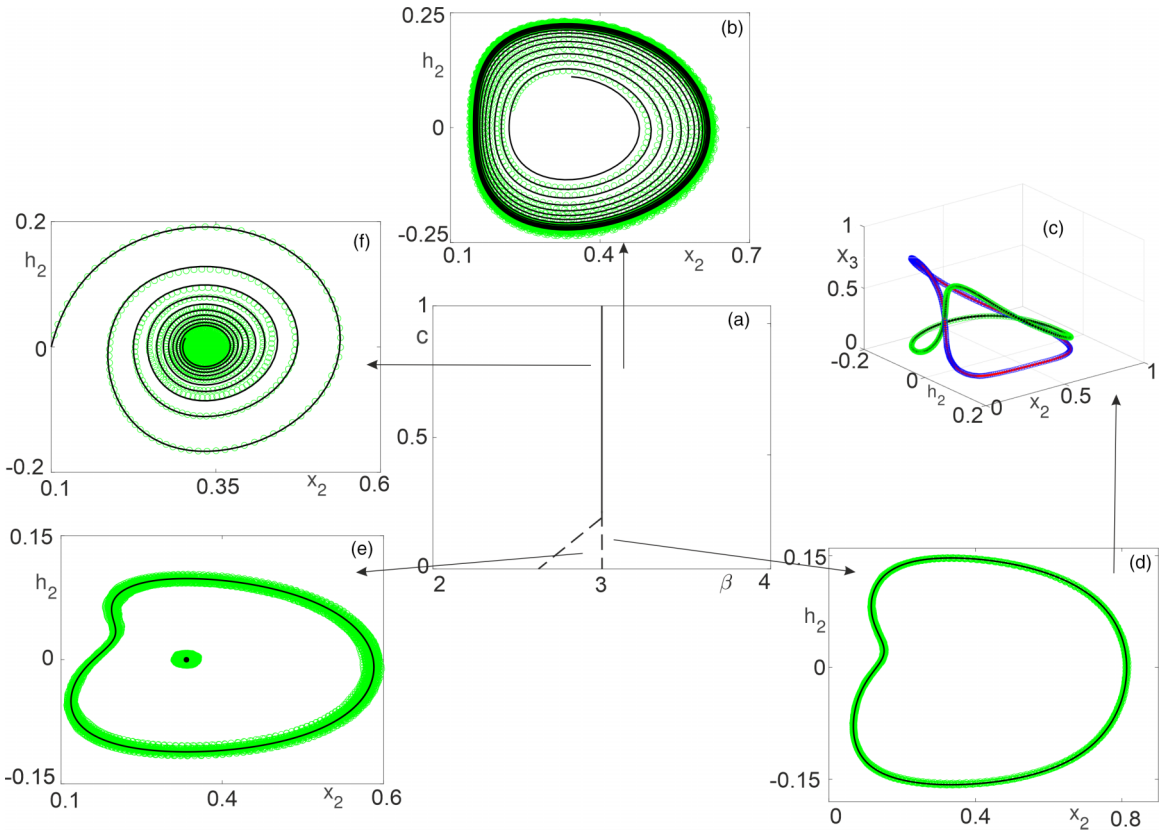

FIG. 4. The behavior of system (29) in the vicinity of the bifurcation line $\beta = 3$. (a) A sketch of a bifurcation diagram illustrating transition from a subcritical to supercritical bifurcation: the vertical line is the line of the double Hopf bifurcation, where broken part shows subcritical behavior and the inclined broken line corresponds to saddle-node bifurcation of cycles. (b)–(e) Phase portraits of some attractors in the vicinity of $\beta = 3$. Black lines represent numerical solutions of (29), while green dots are obtained from fully microscopic stochastic simulations of a system of size $N = 10^5$ spins via the Metropolis-Hastings method.

complex conjugate eigenvalues. These means that the β lies in the interval

$$(2c + 1 - 2\sqrt{c(c+1)})(\nu + 1) < \beta < (2c + 1 + 2\sqrt{c(c+1)})(\nu + 1). \quad (22)$$

The first condition for the Andronov-Hopf bifurcation $\sigma(\beta_0) = 0$ results in $\beta_0 = \nu + 1$. The second condition $\delta(\beta_0) = c > 0$ holds automatically. The nondegeneracy conditions $\mu'(\beta_0) = \sigma'(\beta_0)/2 \neq 0$ and $l_1(\beta_0) \neq 0$ hold at $\nu \neq 2$. Indeed, $2\mu'(\beta_0) = 1/(\nu + 1) > 0$ and the first Lyapunov coefficient for (18) is given by

$$l_1(\beta_0) = \frac{(\nu - 2)(c + 1)}{4c^{\frac{3}{2}}(\nu + 1)} \neq 0, \quad \nu \neq 2. \quad (23)$$

We see that $l_1 \neq 0$ except at $\nu = 2$, when the Andronov-Hopf bifurcation switches from a supercritial to subcritical one.

At $\nu = 2$ the first Lyapunov coefficient vanished and we have that $\beta = 3$ and $\nu = 2$ is the point of the Bautin bifurcation (see, e.g., Ref. [27]). In order to check the nondegeneracy conditions at the point of the Bautin bifurcation we compute the second Lyapunov coefficient for (18) at $\beta = 3$ and $\nu = 2$, which is $l_2 = -\sqrt{c}(c + 1)^2/18 < 0$ for $c > 0$. Consequently, the line $\beta = \nu + 1$ is the line of the Andronov-Hopf bifurcation with the Bautin point at (2,3) that separates the supercritical part of the line from the subcritical one.

In Fig. 3 we demonstrate bifurcation diagram for (18) at $c = 0.01$. The black line is the line of the Andronov-Hopf bifurcation, where continuous part corresponds to supercritical bifurcation and broken part to subcritical one. The green line is the line of saddle-node bifurcation of limit cycles, which is computed numerically with the help of the MATCONT [39]. The star denotes the Bautin point. One can see that parameters space is separated into three regions. Broken black and green lines form a region of multistability, where a stable limit cycle coexists with a stable fixed point. Below solid black and green broken lines the dynamics is defined by a stable fixed point. Above the black line there exists a limit cycle, the correspond to oscillations in both (18) and full stochastic microscopic model.

Finally, let us remark that the Bautin bifurcation for a spin system has been also described in Ref. [40], where a dissipative term in the Curie-Weiss model in presence of local random fields was considered.

D. Feedback Potts model

In the Potts model the lattice variables can assume one of q given states (colors) $s_i = 1 \ldots q$. Variables with equal colors in neighboring sites lower the energy by a factor J and we consider q external fields h_a fixing the relative color fractions $x_a = \frac{1}{N}\sum_i \delta_{s_i,a}$ in the system. The corresponding Hamiltonian

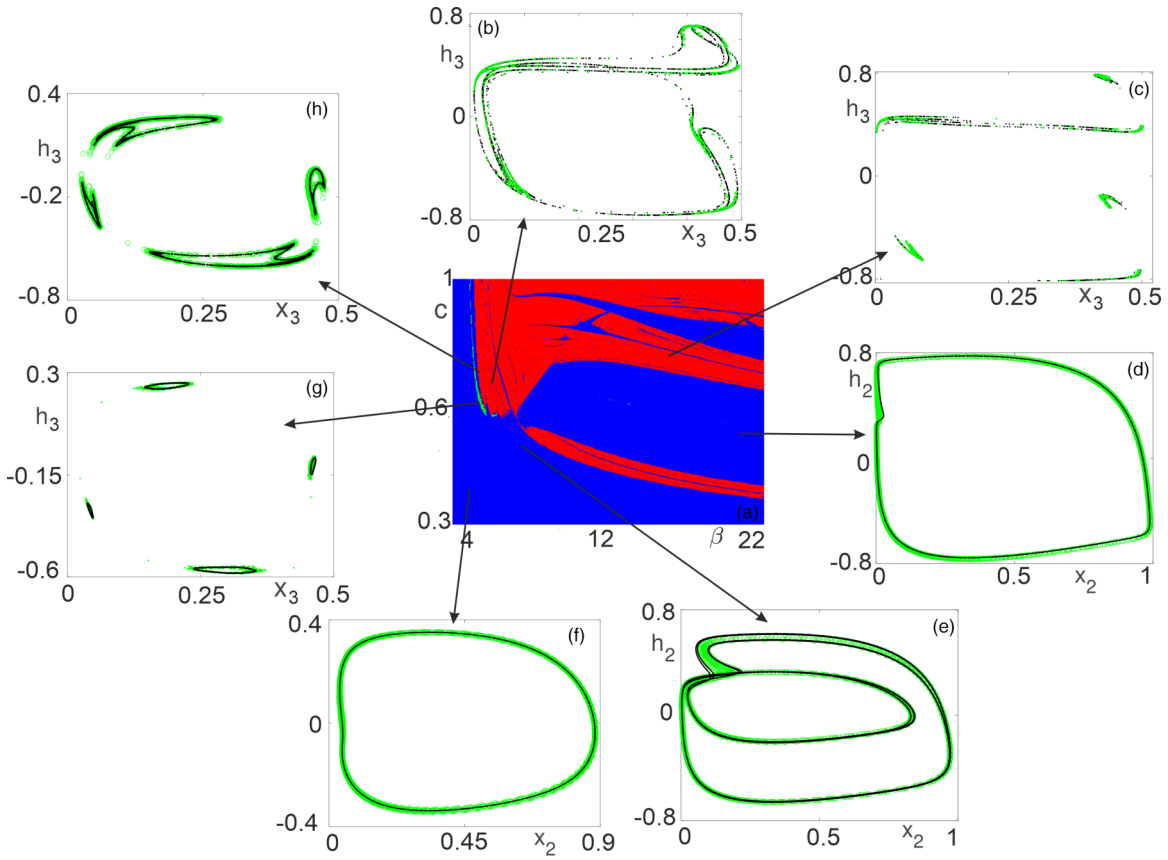

FIG. 5. (a) represents the two-dimensional chart of the Lyapunov exponents for (29), Blue color corresponds to the periodic dynamics, green to quasiperiodic and red to chaotic one. (d)–(f) correspond to the phase portraits of periodic attractors at $\beta = 4$, $c = 0.4$, $\beta = 8.1$, $c = 0.55$, and $\beta = 21$, $c = 0.6$, respectively. In (b), (c), (g), (h) we present Poincaré sections of three chaotic and one quasiperiodic attractors at $\beta = 9.1$, $c = 0.9$, $\beta = 20$, $c = 0.4$, $\beta = 5.2$, $c = 0.65$, and $\beta = 5.1$, $c = 0.75$, respectively. Black lines corresponds to numerical solutions of system (29) and green dots are obtained from fully microscopic stochastic simulations of a system of size $N = 10^6$ spins via the Metropolis-Hastings method.

is

$$H = -J \sum_{\langle i,j \rangle} \delta_{s_i,s_j} - \sum_a h_a \sum_i \delta_{s_i,a}. \tag{24}$$

In the fully connected case the expression for the free energy is given by [41]:

$$A = -\frac{J}{2} \sum_a x_a^2 - \sum_a h_\sigma x_a + T \sum_a x_a \log x_a + \lambda \left(\sum_a x_a - 1 \right), \tag{25}$$

where x_a are the fractions of spins belonging to the same color a and the last term is a Lagrange multiplier enforcing normalization. Following the same scheme used for the Ising model we have that the dynamics will approximately follow the set of equations:

$$\begin{aligned} \dot{x}_a &= -x_a + \frac{e^{\beta(Jx_a + h_a)}}{W}, \\ \dot{h}_a &= -c(x_a - 1/q), \qquad a = 1, \ldots, q, \\ W &= \sum_a e^{\beta(Jx_a + h_a)}, \end{aligned} \tag{26}$$

which describes the motion in the linear response approximation.

System (26) possesses two conservation laws. The first one is

$$\sum_{a=1}^{q} x_a = 1 + C_0 e^{-t}, \tag{27}$$

where C_0 is an arbitrary constant. Since at $t = 0$ the sum of all x_a is equal to 1, we set $C_0 = 0$. With the help of (27) at $C_0 = 0$ we find the second conservation law

$$\sum_{a=1}^{q} h_a = C_1, \tag{28}$$

where C_1 is arbitrary constant. Transformation $h_a \to h_a +$ const results in additional constant term in Hamiltonian (24) and, hence, does not affect the dynamics. Consequently, without loss of generality, we assume that $C_1 = 0$ in (28). Therefore, the first conservation law at $C_0 = 0$ corresponds to the assumption that the number of spins is constant and the second one corresponds to the invariance of the dynamics with respect to constant shifts in the feedback.

Now we consider the case of three colors, i.e., $q = 3$. Taking into account (27) and (28) and rescaling variables as follows $h_a = Jh'_a$, $\beta J = \beta'$, $c/J = c'$ from (26) at $q = 3$ we

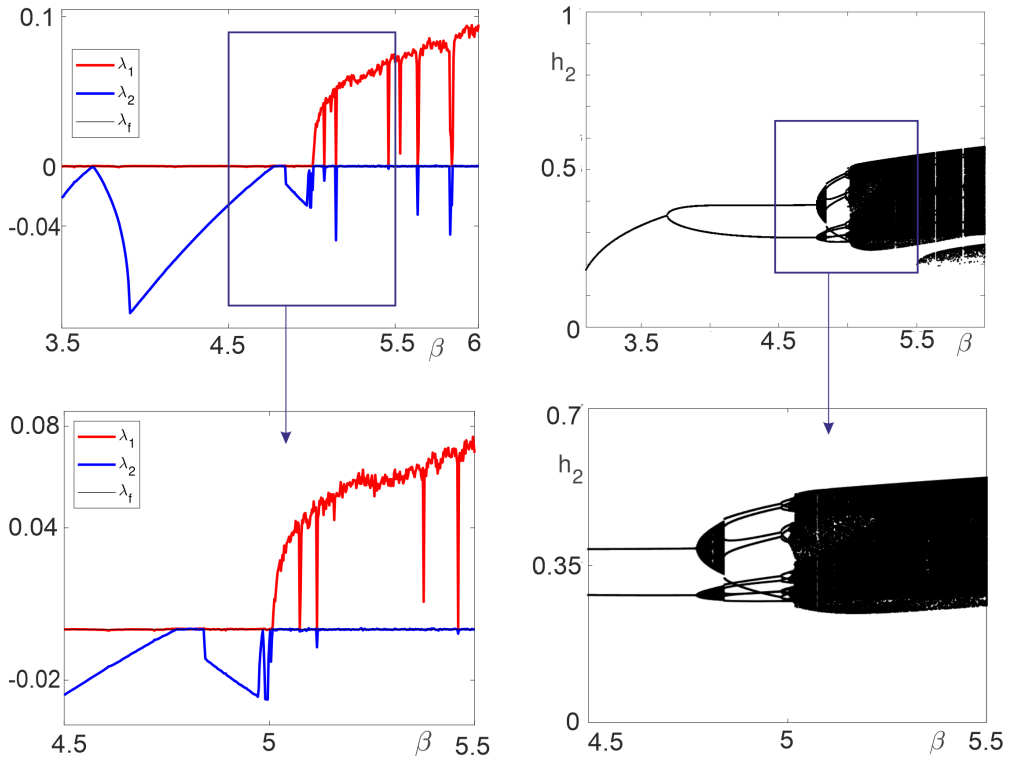

FIG. 6. Lyapunov spectra and bifurcation trees for system (29) at $c = 0.75$ and $\beta \in [3.5, 6]$.

obtain (the primes are omitted)

$$\dot{x}_2 = -x_2 + \frac{e^{\beta(x_2+h_2)}}{\widetilde{W}}, \tag{29}$$

$$\dot{h}_2 = -c\left(x_2 - \frac{1}{3}\right), \tag{30}$$

$$\dot{x}_3 = -x_3 + \frac{e^{\beta(x_3+h_3)}}{\widetilde{W}}, \tag{31}$$

$$\dot{h}_3 = -c\left(x_3 - \frac{1}{3}\right), \tag{32}$$

and

$$\widetilde{W} = e^{\beta(1-x_2-x_3-h_2-h_3)} + e^{\beta(x_2+h_2)} + e^{\beta(x_3+h_3)} \tag{33}$$

System (29) is symmetric with respect to swapping of indices $(2 \longleftrightarrow 3)$ and has one equilibrium point $A = (1/3, 0, 1/3, 0)$. The eigenvalues of the Jacobi matrix at this fixed point are

$$\lambda_{1,2,3,4} = \frac{\beta - 3}{2} \pm \frac{\sqrt{\beta^2 - 6(2c+1)\beta + 9}}{6}. \tag{34}$$

Suppose that

$$\beta \in (3[2c + 1 - 2\sqrt{c^2 + c}], 3[2c + 1 + 2\sqrt{c^2 + c}]), \tag{35}$$

then the eigenvalues are complex conjugated. Passing through $\beta = 3$ the real part of eigenvalues cross the imaginary axis and, hence, the fixed point A losses its stability. Due to the symmetry of (29), the Jacobi matrix at A has multiple eigenvalues and we have the resonant double Hopf bifurcation (see, e.g., Ref. [42] and references therein). Consequently, the analytical treatment of the behavior of (29) near $\beta = 3$ is connected with some difficulties. However, numerically we observe that the dynamics in the vicinity of the bifurcation line $\beta = 3$ is similar to those of the Blume-Capel system near the line of the Andoronov-Hopf bifurcation (see, Fig. 4 and cf. Fig. 3). From Fig. 4 we see that in the lower left part of the bifurcation line $\beta = 3$ there is a region of multistability [see, Figs. 4(e), 4(d)], where a fixed point coexists with a periodic orbit. This suggest that there exists some c^* such that for $c < c^*$ the bifurcation at $\beta = 3$ is subcritical. Increasing the value of c we observe that the bifurcation type switches from subcritical to supercritical one: there is no multistability and at $\beta = 3$ a stable small-amplitude limit cycle is born [see Figs. 4(b), 4(f)]. Let us also remark that due to the symmetry of (29) there are always two coexisting orbits, which can be seen from Figs. 4(c), 4(d).

In order to study possible type of dynamics that appear in (29) away from the line $\beta = 3$ we compute the dependence of the Lyapunov spectrum on the parameters β and c for the region $(\beta, c) \in [3, 5, 22] \times [0.3, 1]$. For computation of the Lyapunov spectrum we use the standard algorithm by Bennetin *et al.* (see Ref. [43]). We present the corresponding two-dimensional chart of Lypaunov exponents in Fig. 5. We color each point in this chart according to the signs of two largest Lyapunov exponents as follows:

(1) $\lambda_1 = 0, 0 > \lambda_2 > \lambda_3 > \lambda_4$: periodic regime and blue color;

(2) $\lambda_1 = \lambda_2 = 0, 0 > \lambda_3 > \lambda_4$: quasiperiodic regime and green color;

(3) $\lambda_1 > 0, \lambda_2 = 0, 0 > \lambda_3 > \lambda_4$: chaotic regime and red color.

In Fig. 5 we also demonstrate phase portraits and Poincaré sections of typical attractors that appear in (29). Throughout

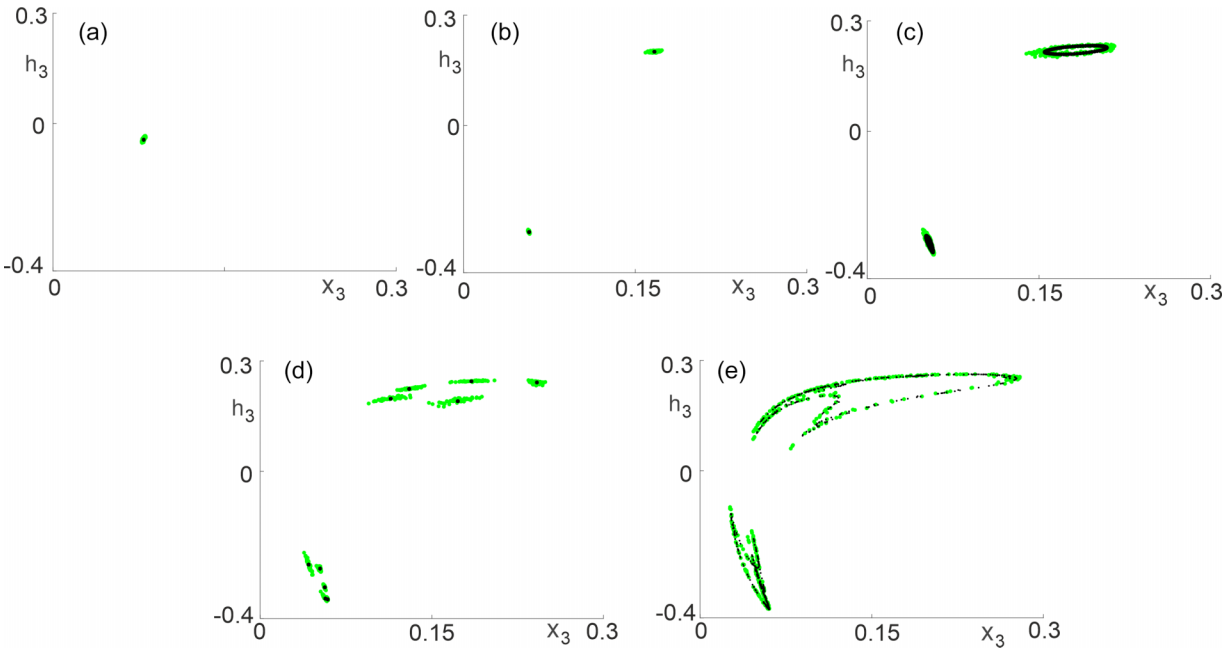

FIG. 7. Poincaré sections of the attractors that appear along the line of the Afraimovich-Shilnikov bifurcation scenario at $c = 0.75$. (a) A stable periodic orbit at $\beta = 3.6$; (b) a stable periodic orbit after period doubling at $\beta = 4.5$; (c) a stable quasiperiodic orbit at $\beta = 4.8$; (d) a resonant periodic orbit at $\beta = 4.9$; (e) a chaotic attractor at $\beta = 5.1$. By black lines we show a numerical solutions of (29) and green dots are obtained from fully microscopic stochastic simulations of a system of size $N = 10^6$ spins via the Metropolis-Hastings method.

this work the Poincaré map is constructed by considering intersections of the flow governed by (29) with the plane $x_2 = 1/2$, if it is not stated otherwise.

The vast blue regions in Fig. 5 correspond to the existence of a stable periodic orbit. There are also two separated red regions of the chaotic dynamics. The appearance of the chaotic attractors in these regions is governed by different scenarios. In the upper left region of Fig. 5 we see a thin green stripe of quasiperiodic dynamics that is adjacent to the thin region of periodic behavior with chaotic one next to it. This suggests that chaotic attractors can appear through the Afraimovich-Shilnikov scenario of an invariant torus destruction (see, e.g., Refs. [28,44,45]).

In the region of lower feedback one can observe a big blue area of periodic oscillations next to a narrow red strip of chaotic ones. From Figs. 5(f), 5(e) one can see that if we approach this red region from the right the period of oscillations increases. Therefore, one can expect the appearance of the cascade of period doubling bifurcations, which we confirm below.

Let us begin with the onset of chaotic oscillations in the upper left part of the bifurcation diagram (see Fig. 5). We see that inside the blue regions adjacent to red one there is a narrow green patch. The left border of this green patch is the line of the supercritical Neimark-Sacker bifurcation (see, e.g., Refs. [27,46,47]), that corresponds to the birth of a stable quasiperiodic regime, which is called an invariant torus. The right border of the green region represents the formation of resonant stable and unstable periodic orbits that appear through the saddle-node bifurcation. Then, if we move further to the right in the bifurcation diagram, the stable resonant orbit becomes chaotic and so-called torus-chaos attractor appears.

We demonstrate realization of this scenario in (29) at $c = 0.75$ and $\beta \in [3.4, 22]$. In Fig. 6 we show the Lyapunov spectra and the bifurcations trees for this region. From Fig. 6(b) one can clearly see that, after one period-doubling bifurcation, a periodic attractor becomes quasiperiodic one, undergoing the supercritical Neimark-Sacker bifurcation. We can observe a narrow but distinct region of the existence of quasiperiodic dynamics in Figs. 6(b), 6(c). Then this quasiperiodic orbit becomes resonant and a long-periodic orbit is born. This resonant periodic orbit becomes chaotic after undergoing a cascade of period doubling bifurcations and a chaotic attractor is born on the basis of former quasiperiodic orbit. We demonstrate Poincaré sections of the attractors along

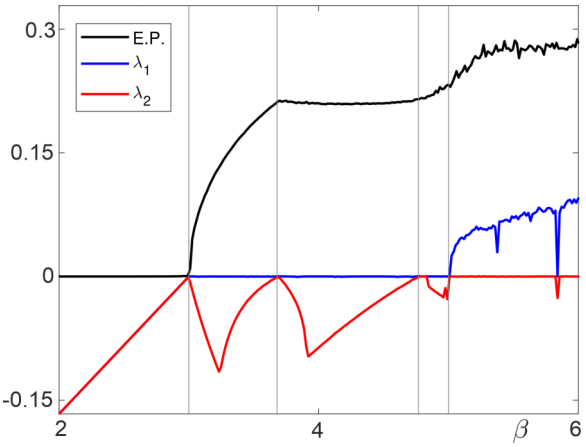

FIG. 8. Entropy production for the Potts model and the Lyapunov spectrum for (29) at $c = 0.75$ and $\beta \in [2, 6]$.

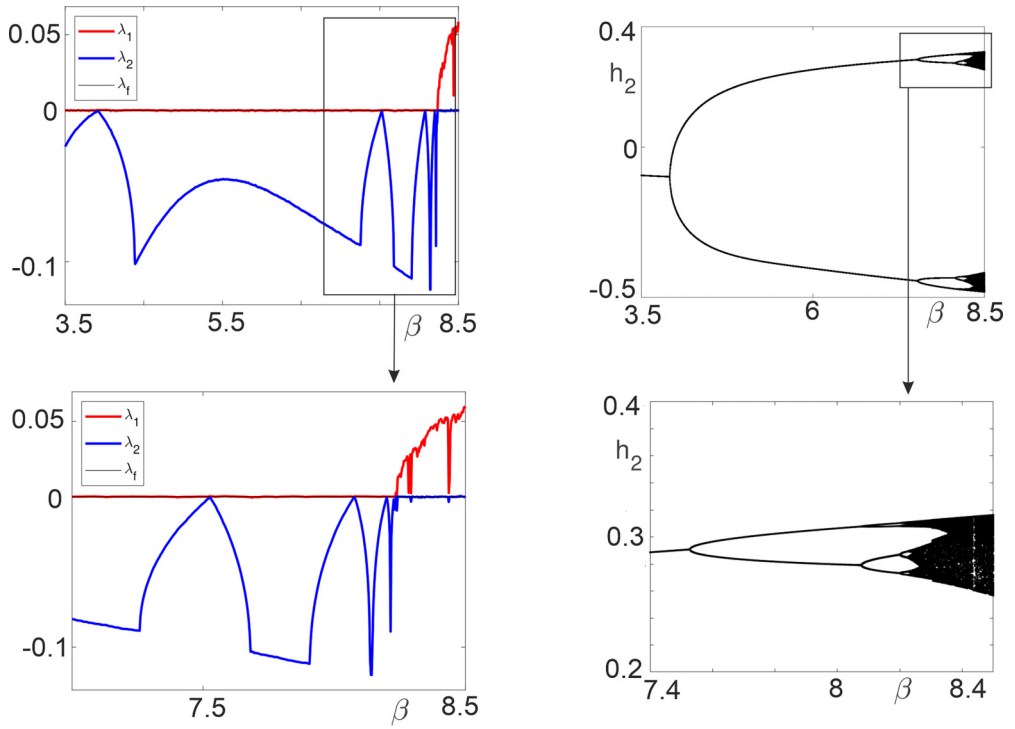

FIG. 9. Lyapunov spectra and bifurcation trees for the Feigenbaum cascade of period doubling in (29) at $c = 0.55$ and $\beta \in [3.1, 8.6]$.

the line of the Afraimovich-Shilnikov bifurcation scenario in Fig. 7.

We also compute the dependence of the entropy production for the Potts model on the parameter β and compare it with those of the Lyapunov spectrum for (29) (see Fig. 8). The average rate of entropy production can be calculated from the out-of-equilibrium definition of work for feedback-driven systems [48,49], for the feedback Potts model we have the formula

$$\sigma = \sum_a \dot{h}_a x_a. \tag{36}$$

From Fig. 8 one can see that the changes in the entropy production are in direct correlation with the bifurcations in the feedback model.

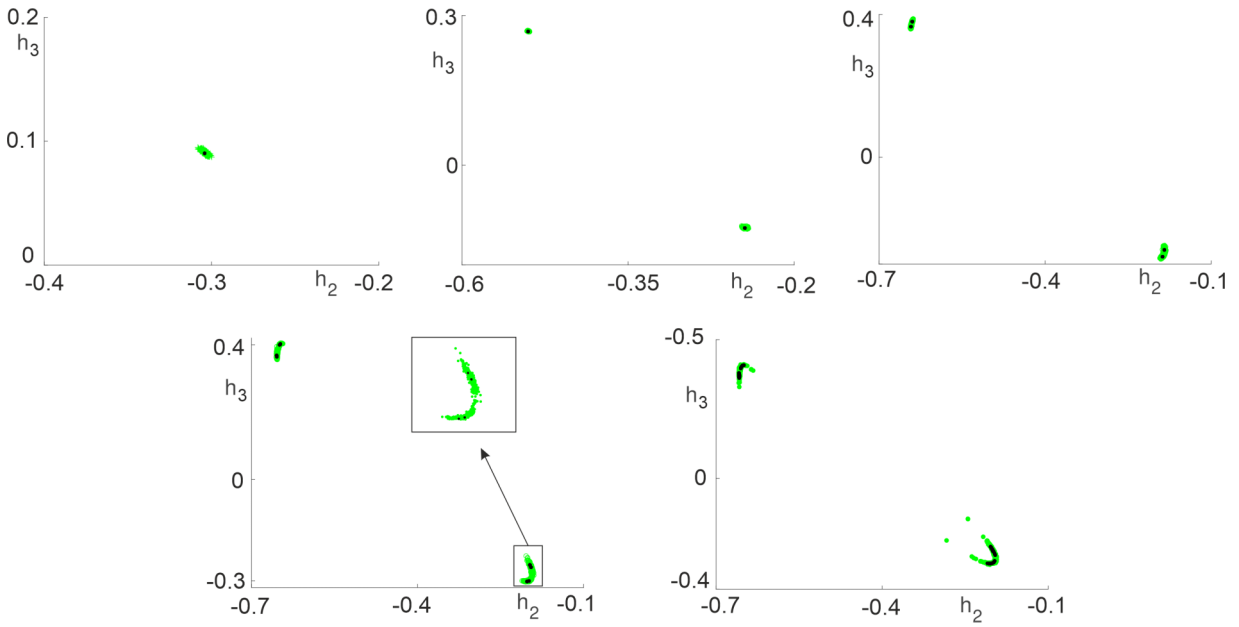

FIG. 10. Poincaré sections of the attractors that appear along the line of the Feigenbaum cascade of period doubling. In all plates $c = 0.55$ and β is 3.5, 4.5, 7.7, 8.1, and 8.3, respectively. Numerical solutions of (29) are given in black, while green dots are obtained from fully microscopic stochastic simulations of a system of size $N = 10^6$ spins via the Metropolis-Hastings method.

Chaotic attractors in (29) can also appear as a result of the Feigenbaum cascade of period doubling. This is typical for the lower part of the bifurcation chart in Fig. 5. We suppose that $c = 0.55$ and $\beta \in [3.1, 8.6]$ and present the corresponding graphs of largest Lyapunov exponents and bifurcation trees in Fig. 9. One can observe a typical cascade of period doubling that a periodic orbit undergoes. We demonstrate Poincaré sections of the attractors along the line of the Feigenbaum scenario in Fig. 10. One can see that period doubling can be observed both in dynamical system (29) and in the microscopic stochastic simulations of a system of size $N = 10^6$ spins. Upon performing simulations of the full many-body system at different sizes we checked that stochastic fluctuations of the Poincaré sections reduce and converge to the predictions of the ODEs.

Finally, it is worth noting that the dynamical system (29) is four dimensional and in principle hyperchaotic dynamics can appear there. However, for the studied regions of the control parameters we have observed only one direction of instability in (29). Moreover, we have not found in these regions of the parameters any other routes to chaotic oscillations apart from those reported above.

III. CONCLUSION

In this work we have analyzed classical spin lattice models, namely the Ising model, the Blume-Capel model, and the Potts model in presence of a negative feedback between the order parameter and the external field(s). These models are representative of the universality classes of equilibrium phase transitions and here we have shown that their usual critical points and phase transition lines get transformed into more complex bifurcations with the emergence of periodic, quasiperiodic, and chaotic oscillatory patterns. At odds with the case of driven systems [17–21] these oscillations are emerging self-oscillations and the system is autonomous, with no explicit dependence on time.

Our first general result is the derivation from linear response theory of simple lower-dimensional dynamical systems that quantitatively reproduce the many-body stochastic simulations for fully connected models. These systems can then be analyzed by classical tools of bifurcation theory.

In some cases the system inherits the main features of its equilibrium counterpart, including analytical tractability. This is the case of the Ising model, where we have shown that in finite dimensions, namely 2D, self-oscillations can emerge with a nontrivial exponent for the amplitude $\beta = 1/8$ [50] in line with the celebrated Onsager solution for the static system.

We have demonstrated that for the Blume-Capel model on a fully connected graph the usual tricritical point gets transformed into the Bautin bifurcation point and the second- and first-order phase transition lines are taken over by subcritical and supercritical Andronov-Hopf bifurcation lines, respectively. These results are independent of the feedback strength parameter c, as soon as this does not break the validity of the continuous approximation, that is valid in the thermodynamic limit and they are nicely summarized qualitatively by the Landau theory of an homogeneous self-compatible field in presence of a feedback.

On the other hand we have shown that for the case of the Potts model with feedback, the dynamical picture is much more complex, due to the increased effective dimensions in which the order and control parameters exist (from two to four in going from the Ising model to the Potts model with $q = 3$ colors). The character of the bifurcation where self-oscillations emerge that substitutes the equilibrium phase transition (at $\beta_c = q$) depends on the strength of the feedback c. For low enough c it is discontinuous (subcritical) and there exists a region where a stable fixed point coexists with self-oscillations. This corresponds well with the static equilibrium transition, that is known to be first-order for the fully connected Potts model at $q = 3$.

However, if one increases c, the amplitude of the emerging self-oscillations decreases up to a certain critical point where it becomes continuous akin to the Bautin bifurcation. This time it depends on the feedback strength and at odds with respect to the underlying free energy landscape. Furthermore, if one increases β (i.e., decreases temperature), we have obtained that the bifurcation diagram of the Potts model with feedback endows complex scenarios with cascades of bifurcations leading to new limit cycles and quasiperiodic attractors and eventually to chaotic ones. The out-of-equilibrium thermodynamic features of these systems have been worked out numerically and we have demonstrated how singularities of the entropy production correspond to qualitative changes in the spectrum of the Lyapunov exponents and the underlying bifurcations.

Among the many future directions of this work we believe it would be interesting to analyze feedback lattice models with generalized out-of-equilibrium Landau functional formalism [51] extending it beyond the Ising systems as well as to apply our framework to data analysis of collective oscillations in natural systems [52], especially synchronization of neuronal systems [53]. Another interesting problem is in regard to the finite-size scaling study of bifurcations as out-of-equilibrium phase transitions in such high-dimensional stochastic systems. This is a well-known topic in equilibrium statistical mechanics [6]. A phenomenological approach, pursued for the Ising model [33], would consist in adding a Langevin noise term to the ODEs, while a more rigorous approach would require us to study the thermodynamic limit, that is where phase transitions are defined more in general [54].

ACKNOWLEDGMENTS

D.D.M., A.P., and M.F.A. thank Professor Enzo Marinari for support and helpful discussions. D.S. is grateful to Alexei Kazakov and Natalia Stankevich for useful discussions. The authors would like to acknowledge the DIPC Supercomputing Center for computational resources and their technical support and assistance. D.S. was supported by the RSF Grant No. 19-71-10048 (Sec. IID).

[1] A. Andronov, A. Vitt, and S. Khaikin, *Theory of Oscillators* (Dover, Mineola, 1966).

[2] S. H. Strogatz, *Nonlinear Dynamics and Chaos with Student Solutions Manual: With Applications to Physics,*

Biology, Chemistry, and Engineering (CRC Press, Boca Raton, 2018).
[3] J. Murray, *Mathematical biology: I. An introduction* (Springer, Berlin, 2002).
[4] L. Landau and E. Lifshitz, *Statistical Physics: V. 5: Course of Theoretical Physics* (Pergamon Press, Oxford, 1969).
[5] V. Pokrovskii and A. Patashinskii, *Fluctuation Theory of Phase Transitions* (Pergamon Press, Oxford, 1979).
[6] J. Cardy, *Scaling and Renormalization in Statistical Physics* (Cambridge University Press, Cambridge, 1996), Vol. 5.
[7] H. Hinrichsen, Adv. Phys. **49**, 815 (2000).
[8] M. Fruchart, R. Hanai, P. B. Littlewood, and V. Vitelli, Nature (London) **592**, 363 (2021).
[9] L. V. Gambuzza, F. Di Patti, L. Gallo, S. Lepri, M. Romance, R. Criado, M. Frasca, V. Latora, and S. Boccaletti, Nat. Commun. **12**, 1255 (2021).
[10] R. Spelat, N. Jihua, C. A. Sánchez Triviño, S. Pifferi, D. Pozzi, M. Manzati, S. Mortal, I. Schiavo, F. Spada, M. E. Zanchetta *et al.*, Cell Death Dis. **13**, 705 (2022).
[11] A. P. Millán, J. J. Torres, and G. Bianconi, Phys. Rev. E **99**, 022307 (2019).
[12] Y. Kuramoto, in *International Symposium on Mathematical Problems in Theoretical Physics* (Springer, Berlin, 1975), pp. 420–422.
[13] K. Sone, Y. Ashida, and T. Sagawa, Phys. Rev. Res. **4**, 023211 (2022).
[14] T. Carletti, L. Giambagli, and G. Bianconi, Phys. Rev. Lett. **130**, 187401 (2023).
[15] A. P. Millán, J. J. Torres, and G. Bianconi, Phys. Rev. Lett. **124**, 218301 (2020).
[16] K. P. O'Keeffe and S. H. Strogatz, Phys. Rev. E **93**, 062203 (2016).
[17] Y. Zhang and A. C. Barato, J. Stat. Mech.: Theory Exp. (2016) 113207.
[18] G. M. Buendia and P. A. Rikvold, Phys. Rev. E **78**, 051108 (2008).
[19] M. Keskin, O. Canko, and Ü. Temizer, Phys. Rev. E **72**, 036125 (2005).
[20] J. Mendes and E. Lage, J. Stat. Phys. **64**, 653 (1991).
[21] D. T. Robb and A. Ostrander, Phys. Rev. E **89**, 022114 (2014).
[22] A. Jenkins, Phys. Rep. **525**, 167 (2013).
[23] J. Guckenheimer and P. Holmes, *Nonlinear Oscillations, Dynamical Systems, and Bifurcations of Vector Fields* (Springer Science & Business Media, Berlin, 2013).
[24] A. Pikovsky, M. Rosenblum, and J. Kurths, in *Synchronization: A Universal Concept in Nonlinear Sciences* (Cambridge University Press, Cambridge, 2001), Vol. 2, p. 3 .
[25] O. E. Rössler and C. Letellier, *Chaos: The World of Nonperiodic Oscillations* (Springer Nature, 2020), p. 55.
[26] R. M. Borisyuk and A. B. Kirillov, Biol. Cybern. **66**, 319 (1992).
[27] Y. Kuznetsov, *Elements of Applied Bifurcation Theory* (Springer, New York, 1998), Vol. 42.
[28] I. Garashchuk, D. Sinelshchikov, A. Kazakov, and N. Kudryashov, Chaos **29**, 063131 (2019).
[29] I. Garashchuk, A. Kazakov, and D. Sinelshchikov, Nonlin. Dyn. **101**, 1199 (2020).
[30] I. Garashchuk and D. Sinelshchikov, Chaos **31**, 023130 (2021).
[31] A. Shykhmamedov, E. Karatetskaia, A. Kazakov, and N. Stankevich, Nonlinearity **36**, 3501 (2023).
[32] R. J. Baxter, *Exactly Solved Models in Statistical Mechanics* (Elsevier, Amsterdam, 2016).
[33] D. De Martino, J. Phys. A: Math. Theor. **52**, 045002 (2019).
[34] N. Metropolis, A. W. Rosenbluth, M. N. Rosenbluth, A. H. Teller, and E. Teller, J. Chem. Phys. **21**, 1087 (1953).
[35] W. Hastings, Biometrika **57**, 97 (1970).
[36] R. Zwanzig, *Nonequilibrium Statistical Mechanics* (Oxford University Press, Oxford, 2001).
[37] L. Onsager, Phys. Rev. **65**, 117 (1944).
[38] M. Blume, Phys. Rev. **141**, 517 (1966).
[39] A. Dhooge, W. Govaerts, Y. Kuznetsov, H. Meijer, and B. Sautois, Math. Comput. Modell. Dyn. Syst. **14**, 147 (2008).
[40] F. Collet and M. Formentin, J. Stat. Phys. **176**, 478 (2019).
[41] F.-Y. Wu, Rev. Mod. Phys. **54**, 235 (1982).
[42] H. Broer, H. Hanßmann, and F. Wagener, Indagationes Math. **32**, 33 (2021).
[43] G. Benettin, L. Galgani, A. Giorgilli, and J.-M. Strelcyn, Meccanica **15**, 9 (1980).
[44] V. S. Afraimovich and L. P. Shilnikov, Am. Math. Soc. Transl. **149**, 201 (1991).
[45] I. Sataev and N. Stankevich, Chaos **31**, 023140 (2021).
[46] L. O. Chua, L. P. Shilnikov, A. L. Shilnikov, and D. V. Turaev, *Methods of Qualitative Theory in Nonlinear Dynamics (Part II)* (World Scientific, Singapore, 2001), Vol. 5.
[47] G. Iooss, *Bifurcation of Maps and Applications* (Elsevier, Amsterdam, 1979).
[48] T. Sagawa and M. Ueda, Phys. Rev. E **85**, 021104 (2012).
[49] D. De Martino and A. C. Barato, Phys. Rev. E **100**, 062123 (2019).
[50] As usual this shall not be confused with the inverse temperature.
[51] L. Guislain and E. Bertin, Phys. Rev. Lett. **130**, 207102 (2023).
[52] F. Lombardi, S. Pepić, O. Shriki, G. Tkačik, and D. De Martino, Nat. Comput. Sci. **3**, 254 (2023).
[53] F. Lombardi, S. Pepić, O. Shriki, G. Tkačik, and D. De Martino, Nature Comput. Sci. 1 (2023).
[54] D. Ruelle, *Statistical Mechanics: Rigorous Results* (World Scientific, Singapore, 1969).